4

CCD imaging

This chapter will deal with the most basic use of a CCD, that of direct imaging. We will discuss a few more preliminaries such as flat fields, the calculation of gain and read noise for a CCD, and how the signal-to-noise value for a measurement is determined. The chapter then continues by providing a brief primer on the use of calibration frames in standard two-dimensional CCD data image reduction. Finally, we cover some aspects of CCD imaging itself including applications of wide-field imaging with CCD mosaics and CCD drift scanning.

4.1 Image or plate scale

One of the basic parameters of importance to a CCD user is that of knowing the plate scale of your image. Plate scale is a term that originates from when photographic plates were used as the main imaging device and is often given in arcsec/mm. For a CCD user, however, a more convenient unit for the plate scale is arcsec/pixel. Clearly the conversion from one to the other is simple.

The focal ratio of a telescope is given by

$$f/ = \frac{\text{focal length of primary mirror}}{\text{primary mirror diameter}},$$

where both values are in the same units and "primary mirror" would be replaced by "primary objective lens" for a refractor. Taking the focal length of the primary (f) in mm and the CCD pixel size (μ) in microns, we can calculate the CCD plate scale as

$$P = \frac{206\,265 \times \mu}{1000 \times f} \quad \text{(arcsec/pixel)},$$

https://doi.org/10.1017/CBO9780511807909.006

where 206 265 is the number of arcseconds in 1 radian and 1000 is the conversion factor between millimeters and microns.

For a 1-m telescope of $f/ = 7.5$, the focal length (f) of the primary would be 7500 mm. If we were to use a Loral CCD with 15-micron pixels as an imager, the above expression would yield an image scale on the CCD of 0.41 arcsec/pixel. This image scale is usually quite a good value for direct imaging applications for which the seeing is near 1 or so arcseconds.

There are times, however, when the above expression for the plate scale of a CCD may not provide an accurate value. This could occur if there are additional optics within the instrument that change the final *f*-ratio in some unknown manner. Under these conditions, or simply as an exercise to check the above calculation, one can determine the CCD plate scale observationally. Using a few CCD images of close optical double stars with known separations (e.g., the Washington Double Star Catalog – http://ad.usno.navy.mil/wds/), measurement of the center positions of the two stars and application of a bit of plane geometry will allow an accurate determination of the pixel-to-pixel spacing, and hence the CCD plate scale. This same procedure also allows one to measure the rotation of the CCD with respect to the cardinal directions using known binary star position angles.

4.2 Flat fielding

To CCD experts, the term "flat field" can cause shivers to run up and down their spine. For the novice, it is just another term to add to the lexicon of CCD jargon. If you are in the latter category, don't be put off by these statements but you might want to take a minute and enjoy your thought of "How can a flat field be such a big deal?" In principle, obtaining flat field images and flat fielding a CCD image are conceptually easy to understand, but in practice the reality that CCDs are not perfect imaging devices sets in.

The idea of a flat field image is simple. Within the CCD, each pixel has a slightly different gain or QE value when compared with its neighbors. In order to flatten the relative response for each pixel to the incoming radiation, a flat field image is obtained and used to perform this calibration. Ideally, a flat field image would consist of uniform illumination of every pixel by a light source of identical spectral response to that of your object frames. That is, you want the flat field image to be spectrally and spatially flat. Sounds easy, doesn't it? Once a flat field image is obtained, one then simply divides each object frame by it and voilà: instant removal of pixel-to-pixel variations.

Before talking about the details of the flat fielding process and why it is not so easy, let us look at the various methods devised to obtain flat field exposures with a CCD. All of these methods involve a light source that is brighter than any astronomical image one would observe. This light source provides a CCD calibration image of high signal-to-noise ratio. For imaging applications, one very common procedure used to obtain a flat field image is to illuminate the inside of the telescope dome (or a screen mounted on the inside of the dome) with a light source, point the telescope at the bright spot on the dome, and take a number of relatively short exposures so as not to saturate the CCD. Since the pixels within the array have different responses to different colors of light, flat field images need to be obtained through each filter that is to be used for your object observations. As with bias frames discussed in the last chapter, five to ten or more flats exposed in each filter should be obtained and averaged together to form a final or master flat field, which can then be used for calibration of the CCD. Other methods of obtaining a CCD flat field image include taking CCD exposures of the dawn or dusk sky or obtaining spatially offset images of the dark night sky; these can then be median filtered to remove any stars that may be present (Tyson, 1990; Gilliland, 1992; Massey & Jacoby, 1992; Tobin, 1993).

To allow the best possible flat field images to be obtained, many observatories have mounted a flat field screen on the inside of each dome and painted this screen with special paints (Massey & Jacoby, 1992) that help to reflect all incident wavelengths of light as uniformly as possible. In addition, most instrument user manuals distributed by observatories discuss the various methods of obtaining flat field exposures that seem to work best for their CCD systems. Illumination of dome flat field screens has been done by many methods, from a normal 35-mm slide projector, to special "hot filament" quartz lamps, to various combinations of lamps of different color temperature and intensity mounted like headlamps on the front of the telescope itself. Flat fields obtained by observation of an illuminated dome or dome screen are referred to as dome flats, while observations of the twilight or night sky are called sky flats.

A new generation of wide-field imagers and fast focal length telescopes presents some problems for the normal "dome" screen approach to flat fielding. To achieve large-scale, uniform flat fields Zhou *et al.* (2004) have developed a method by which an isotropic diffuser is placed in front of the telescope and illuminated by reflected light from the dome screen. They claim to obtain flat fields with a measurement of the detector inhomogeneities as good as supersky flats over a 1° field of view. Shi and Wang (2004) discuss flat fielding for a wide field multi-fiber spectroscopic telescope. They use

https://doi.org/10.1017/CBO9780511807909.006

a combination of fiber lamp flat fields and offset sky flats to calibrate the pixel-to-pixel variations.

CCD imaging and photometric applications use dome or sky flats as a means of calibrating out pixel-to-pixel variations. For spectroscopic applications, flat fields are obtained via illumination of the spectrograph slit with a quartz or other high intensity projector lamp housed in an integrating sphere (Wagner, 1992). The output light from the sphere attempts to illuminate the slit, and thus the grating of the spectrograph, in a similar manner to that of the astronomical object of interest. This type of flat field image is called a projector flat. While the main role of a flat field image is to remove pixel-to-pixel variations within the CCD, these calibration images will also compensate for any image vignetting and for time-varying dust accumulation, which may occur on the dewar window and/or filters within the optical path.

Well, so far so good. So what is the big deal about flat field exposures? The problems associated with flat field images and why they are a topic discussed in hushed tones in back rooms may still not be obvious to the reader. There are two major concerns. One is that uniform illumination of every CCD pixel (spatially flat) to one part in a thousand is often needed but in practice is very hard to achieve. Second, QE variations within the CCD pixels are wavelength dependent. This wavelength dependence means that your flat field image should have the exact wavelength distribution over the band-pass of interest (spectrally flat) as that of each and every object frame you wish to calibrate. Quartz lamps and twilight skies are not very similar at all in color temperature (i.e., spectral shape) to that of a dark nighttime sky filled with stars and galaxies.[1] Sky flats obtained of the dark nighttime sky would seem to be our savior here, but these types of flat fields require long exposures to get the needed signal-to-noise ratio and multiple exposures with spatial offsets to allow digital filtering (e.g., median) to be applied in order to remove the stars. In addition, the time needed to obtain (nighttime) sky flats is likely not available to the observer who generally receives only a limited stay at the telescope. Thus, whereas very good calibration data lead to very good final results, the fact is that current policies of telescope scheduling often mean that we must somehow compromise the time used for calibration images with that used to collect the astronomical data of interest. Modern telescopes often observe in queue mode or service mode thereby removing the "at the telescope" interaction of the observer whose data are being collected from the data collection process itself. Often the calibration frames desired are not what is obtained.

[1] One good sky region for twilight flats has been determined to be an area 13° east of zenith just after sunset (Chromey & Hasselbacher, 1996).

Flat fielding satellite CCD imagers (such as those on HST) and space misions (such as Cassini) are often hard to achieve in practice. Laboratory flat fields taken prior to launch are often used as defaults for science observations taken in orbit. Defocused or scanned observations of the bright Earth or Moon are often used for these. Dithered observations of a star field can be used as well in a slightly different way. Multiple observations of the same (assumed constant) stars as they fall on different pixels are used to determine the relative changes in brightness and thus map out low frequency variations in the CCD. An example of such a program is discussed in Mack *et al.* (2002).

Within the above detailed constraints on a flat field image, it is probably the case that obtaining a perfect, color-corrected flat field is an impossibility. But all is not lost. Many observational projects do not require total perfection of a flat field over all wavelengths or over the entire two-dimensional array. Stellar photometry resulting in differential measurements or on-band/off-band photometry searching for particular emission lines are examples for which one only needs to have good flat field information over small spatial scales on the CCD. However, a project with end results of absolute photometric calibration over large spatial extents (e.g., mapping of the flux distribution within the spiral arms of an extended galaxy) does indeed place stringent limits on flat fielding requirements. For such demanding observational programs, some observers have found that near-perfect flats can be obtained through the use of a combination of dome and sky flats. This procedure combines the better color match and low-spatial frequency information from the dark night sky with the higher signal-to-noise, high spatial frequency information of a dome flat. Experimentation to find the best method of flat fielding for a particular telescope, CCD, and filter combination, as well as for the scientific goals of a specific project, is highly recommended.

A summary of the current best wisdom on flat fields depends on who you talk to and what you are trying to accomplish with your observations. The following advice is one person's view.

What does the term "a good flat field" mean? An answer to that question is: a good flat field allows a measurement to be transformed from its instrumental values into numeric results in a standard system that results in an answer that agrees with other measurements made by other observers. For example, if two observers image the same star, they both observe with a CCD using a V filter, and they each end up with the final result of $V = 14.325$ magnitudes in the Johnson system then, assuming this is an accurate result, one may take this as an indication of the fact that each observer used correct data reduction and analysis procedures (including their flat fielding) for the observations.

https://doi.org/10.1017/CBO9780511807909.006

The above is one way to answer the question, but it still relies on the fact that observers need to obtain good flat fields. Without them, near perfect agreement of final results is unlikely. While the ideal flat field would uniformly illuminate the CCD such that every pixel would receive equal amounts of light in each color of interest, this perfect image is generally not produced with dome screens, the twilight sky, or projector lamps within spectrographs. This is because good flat field images are all about color terms. That is, the twilight sky is not the same color as the nighttime sky, neither of which are the same color as a dome flat. If you are observing red objects, you need to worry more about matching the red color in your flats; for blue objects you worry about the blue nature of your flats. Issues to consider include the fact that if the Moon is present, the sky is bluer then when the Moon is absent, dome flats are generally reddish due to their illumination by a quartz lamp of relatively low filament temperature, and so on. Thus, just as in photometric color transformations, the color terms in flat fields are all important. One needs to have a flat field that is good, as described above, plus one that also matches the colors of interest to the observations at hand.

Proper techniques for using flat fields as calibration images will be discussed in Section 4.5. Modern CCDs generally have pixels that are very uniform, especially the new generation of thick, front-side devices. Modern thinning processes result in more even thickness across a CCD reaching tolerances of 1-2 microns in some cases. Thus, at some level flat fielding appears to be less critical today but the advances resulting in lower overall noise performance provide a circular argument placing more emphasis on high quality flats. Appendix A offers further reading on this subject and the material presented in Djorgovski (1984), Gudehus (1990), Tyson (1990), and Sterken (1995) is of particular interest concerning flat fielding techniques.

4.3 Calculation of read noise and gain

We have talked about bias frames and flat field images in the text above and now wish to discuss the way in which these two types of calibration data may be used to determine the read noise and gain for a CCD.

Noted above, when we discussed bias frames, was the fact that a histogram of such an image (see Figure 3.8) should produce a Gaussian distribution with a width related to the read noise and the gain of the detector. Furthermore, a similar relation exists for the histogram of a typical flat field image (see Figure 4.1). The mean level in the flat field shown in Figure 4.1

https://doi.org/10.1017/CBO9780511807909.006

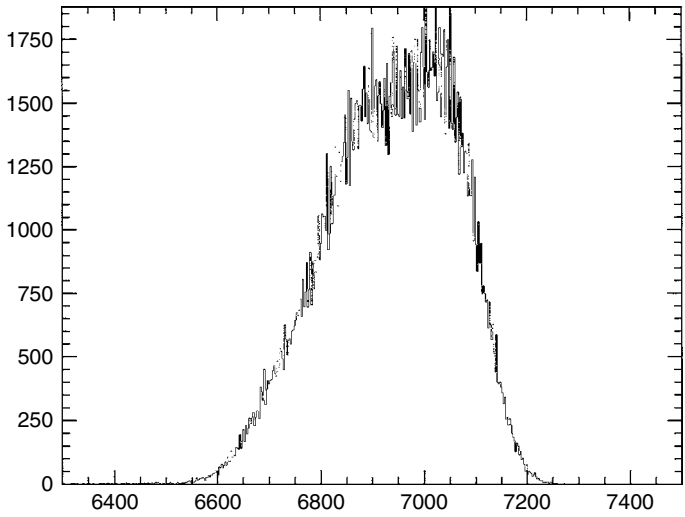

Fig. 4.1. Histogram of a typical flat field image. Note the fairly Gaussian shape of the histrogram and the slight tail extending to lower values. For this R-band image, the filter and dewar window were extremely dusty leading to numerous out of focus "doughnuts" (see Figure 4.4), each producing lower than average data values.

is $\bar{F} = 6950$ ADU and its width (assuming it is perfectly Gaussian (Massey & Jacoby, 1992)) will be given by

$$\sigma_{\mathrm{ADU}} = \frac{\sqrt{\bar{F} \cdot \mathrm{Gain}}}{\mathrm{Gain}}.$$

We have made the assumption in this formulation that the Poisson noise of the flat field photons themselves is much greater than the read noise. This is not unreasonable at all given the low values of read noise in present day CCDs.

Let us now look at how bias frames and flat field images can be used to determine the important CCD properties of read noise and gain. Using two bias frames and two equal flat field images, designated 1 and 2, we can proceed as follows. Determine the mean pixel value within each image.[1] We will call the mean values of the two bias frames $\bar{B}_1$ and $\bar{B}_2$ and likewise $\bar{F}_1$ and $\bar{F}_2$ will be the corresponding values for the two flats. Next, create two difference images ($B_1 - B_2$ and $F_1 - F_2$) and measure the standard deviation

[1] Be careful here not to use edge rows or columns, which might have very large or small values due to CCD readout properties such as amplifier turn on/off (which can cause spikes). Also, do not include overscan regions in the determination of the mean values.

of these image differences: $\sigma_{B_1-B_2}$ and $\sigma_{F_1-F_2}$. Having done that, the gain of your CCD can be determined from the following:

$$\text{Gain} = \frac{(\bar{F}_1 + \bar{F}_2) - (\bar{B}_1 + \bar{B}_2)}{\sigma^2_{F_1-F_2} - \sigma^2_{B_1-B_2}},$$

and the read noise can be obtained from

$$\text{Read noise} = \frac{\text{Gain} \cdot \sigma_{B_1-B_2}}{\sqrt{2}}.$$

4.4 Signal-to-noise ratio

Finally we come to one of the most important sections in this book, the calculation of the signal-to-noise (S/N) ratio for observations made with a CCD.

Almost every article written that contains data obtained with a CCD and essentially every observatory user manual about CCDs contains some version of an equation used for calculation of the S/N of a measurement. S/N values quoted in research papers, for example, do indeed give the reader a feel for the level of goodness of the observation (i.e., a S/N of 100 is probably good while a S/N of 3 is not), but rarely do the authors discuss how they performed such a calculation.

The equation for the S/N of a measurement made with a CCD is given by

$$\frac{\text{S}}{\text{N}} = \frac{N_*}{\sqrt{N_* + n_{\text{pix}}(N_S + N_D + N_R^2)}},$$

unofficially named the "CCD Equation" (Mortara & Fowler, 1981). Various formulations of this equation have been produced (e.g., Newberry (1991) and Gullixson (1992)), all of which yield the same answers of course, if used properly. The "signal" term in the above equation, N_*, is the total number of photons[1] (signal) collected from the object of interest. N_* may be from one pixel (if determining the S/N of a single pixel as sometimes is done for a background measurement), or N_* may be from several pixels, such as all of those contained within a stellar profile (if determining the S/N for the

[1] Throughout this book, we have and will continue to use the terms photons and electrons interchangeably when considering the charge collected by a CCD. In optical observations, every photon that is collected within a pixel produces a photoelectron; thus they are indeed equivalent. When talking about observations, it seems logical to talk about star or sky photons, but for dark current or read noise discussions, the number of electrons measured seems more useful.

measurement of a star), or N_* may even be from say a rectangular area of X by Y pixels (if determining the S/N in a portion of the continuum of a spectrum).

The "noise" terms in the above equation are the square roots of N_*, plus $n_{\rm pix}$ (the number of pixels under consideration for the S/N calculation) times the contributions from N_S (the total number of photons per pixel from the background or sky), N_D (the total number of dark current electrons per pixel), and N_R^2 (the total number of electrons per pixel resulting from the read noise.[1]

For those interested in more details of each of these noise terms, how they are derived, and why each appears in the CCD Equation, see Merline & Howell (1995). In our short treatise, we will remark on some of the highlights of that paper and present an improved version of the CCD Equation. However, let's first make sense out of the equation just presented.

For sources of noise that behave under the auspices of Poisson statistics (which includes photon noise from the source itself), we know that for a signal level of N, the associated 1 sigma error (1σ) is given by $\sqrt{N}$. The above equation for the S/N of a given CCD measurement of a source can thus be seen to be simply the signal (N_*) divided by the summation of a number of Poisson noise terms. The $n_{\rm pix}$ term is used to apply each noise term on a per pixel basis to all of the pixels involved in the S/N measurement and the N_R term is squared since this noise source behaves as shot noise, rather than being Poisson-like (Mortara & Fowler, 1981). We can also see from the above equation that if the total noise for a given measurement $\sqrt{N_* + n_{\rm pix}(N_S + N_D + N_R^2)}$ is dominated by the first noise term, N_* (i.e., the noise contribution from the source itself), then the CCD Equation becomes

$$\frac{\rm S}{\rm N} = \frac{N_*}{\sqrt{N_*}} = \sqrt{N_*},$$

yielding the expected result for a measurement of a single Poisson behaved value.

This last result is useful as a method of defining what is meant by a "bright" source and a "faint" source. As a working definition, we will use the term bright source to mean a case for which the S/N errors are dominated by the source itself (i.e., ${\rm S/N} \sim \sqrt{N_*}$), and we will take a faint source to be the case in which the other error terms are of equal or greater significance compared with N_*, and therefore the complete error equation (i.e., the CCD Equation) is needed.

[1] Note that this noise source is not a Poisson noise source but a shot noise; therefore it enters into the noise calculation as the value itself, not the square root of the value as Poisson noise sources do.

https://doi.org/10.1017/CBO9780511807909.006

The CCD Equation above provides the formulation for a S/N calculation given typical conditions and a well-behaved CCD. For some CCD observations, particularly those that have high background levels, faint sources of interest, poor spatial sampling, or large gain values, a more complete version of the error analysis is required. We can write the complete CCD Equation (Merline & Howell, 1995) as

$$\frac{\mathrm{S}}{\mathrm{N}} = \frac{N_*}{\sqrt{N_* + n_{\mathrm{pix}}\left(1 + \frac{n_{\mathrm{pix}}}{n_B}\right)\left(N_S + N_D + N_R^2 + G^2\sigma_f^2\right)}}.$$

This form of the S/N equation is essentially the same as that given above, but two additional terms have been added. The first term, $(1 + n_{\mathrm{pix}}/n_B)$, provides a measure of the noise incurred as a result of any error introduced in the estimation of the background level on the CCD image. The term n_B is the total number of background pixels used to estimate the mean background (sky) level. One can see that small values of n_B will introduce the largest error as they will provide a poor estimate of the mean level of the background distribution. Thus, very large values of n_B are to be preferred but clearly some trade-off must be made between providing a good estimate of the mean background level and the use of pixels from areas on the CCD image that are far from the source of interest or possibly of a different character.

The second new term added into the complete S/N equation accounts for the error introduced by the digitization noise within the A/D converter. From our discussion of the digitization noise in Chapter 3, we noted that the error introduced by this process can be considerable if the CCD gain has a large value. In this term, $G^2\sigma_f^2$, G is the gain of the CCD (in electrons/ADU) and σ_f is an estimate of the 1 sigma error introduced within the A/D converter[1] and has a value of approximately 0.289 (Merline & Howell, 1995).

In practice for most CCD systems in use and for most observational projects, the two additional terms in the complete S/N equation are often very small error contributors and can be ignored. In the instances for which they become important – for example, cases in which the CCD gain has a high value (e.g., 100 electrons/ADU), the background level can only be estimated with a few pixels (e.g., less than 200), or the CCD data are of poor pixel

[1] The parameter σ_f^2 and its value depend on the actual internal electrical workings of a given A/D converter. We assume here that for a charge level that is half way in between two output ADU steps (that is, 1/2 of a gain step), there is an equal chance that it will be assigned to the lower or to the higher ADU value when converted to a digital number. See Merline & Howell (1995) for further details.

sampling (see Section 5.9) – ignoring these additional error terms will lead to an overestimation of the S/N value obtained from the CCD data.

Let us work through an example of a S/N calculation given the following conditions. A 300-second observation is made of an astronomical source with a CCD detector attached to a 1-m telescope. The CCD is a Thomson 1024×1024 device with 19-micron pixels and it happens that in this example the telescope has a fast f-ratio such that the plate scale is 2.6 arcsec/pixel.[1] For this particular CCD, the read noise is 5 electrons/pixel/read, the dark current is 22 electrons/pixel/hour, and the gain (G) is 5 electrons/ADU. Using 200 background pixels surrounding our object of interest from which to estimate the mean background sky level, we take a mean value for N_B of 620 ADU/pixel. We will further assume here (for simplicity) that the CCD image scale is such that our source of interest falls completely within 1 pixel (good seeing!) and that after background subtraction (see Section 5.1), we find a value for N_* of 24 013 ADU. Ignoring the two additional minor error terms discussed above (as the gain is very small and $n_B = 200$ is quite sufficient in this case), we can write the CCD Equation as

$$\frac{\mathrm{S}}{\mathrm{N}} = \frac{24\,013(\mathrm{ADU}) \cdot G}{\sqrt{24\,013(\mathrm{ADU}) \cdot G + (1) \cdot (620(\mathrm{ADU}) \cdot G + 1.8 + 5^2(e^-))}}.$$

Note that all of the values used in the calculation of the S/N are in electrons, *not* in ADUs. The S/N value calculated for this example is ~342, a very high S/N. With such a good S/N measurement, one might suspect that this is a bright source. If we compare $\sqrt{N_*}$ with all the remaining error terms, we see that indeed this measurement has its noise properties dominated by the Poisson noise from the source itself and the expression $\mathrm{S/N} \sim \sqrt{N_*} = 346$ works well here.

While the S/N of a measurement is a useful number to know, at times we would prefer to quote a standard error for the measurement as well. Using the fact that $\mathrm{S/N} = 1/\sigma$, where σ is the standard deviation of the measurement, we can write

$$\sigma_{\mathrm{magnitudes}} = \frac{1.0857\sqrt{N_* + p}}{N_*}.$$

In this expression, p is equal to $n_{\mathrm{pix}}(1 + n_{\mathrm{pix}}/n_B)(N_S + N_D + N_R^2 + G^2\sigma_f^2)$, the same assumptions apply concerning the two "extra" error terms, and the value of 1.0857 is the correction term between an error in flux (electrons) and that same error in magnitudes (Howell, 1993). We again see that if the Poisson error of N_* itself dominates, the term p can be ignored and this equation

[1] Using the results from Section 4.1, what would be the f-ratio of this telescope?

reduces to that expected for a 1σ error estimate in the limiting case of a bright object.

Additionally, one may be interested in a prediction of the S/N value likely to be obtained for a given CCD system and integration time. N_* is really $N \cdot t$, where N is the count rate in electrons (photons) per second (for the source of interest) and t is the CCD integration time. Noting that the integration time is implicit in the other quantities as well, we can write the following (Massey, 1990):

$$\frac{\mathrm{S}}{\mathrm{N}} = \frac{Nt}{\sqrt{Nt + n_{\mathrm{pix}}\left(N_S t + N_D t + N_R^2\right)}},$$

in which we have again ignored the two minor error terms. This equation illustrates a valuable rule of thumb concerning the S/N of an observation: $\mathrm{S/N} \propto \sqrt{t}$, not to t itself. Solving the above expression for t we find

$$t = \frac{-B + (B^2 - 4AC)^{1/2}}{2A},$$

where $A = N^2$, $B = -(\mathrm{S/N})^2(N + n_{\mathrm{pix}}(N_S + N_D))$, and $C = -(S/N)^2\ n_{\mathrm{pix}} N_R^2$. Most instrument guides available at major observatories provide tables that list the count rate expected for an ideal star (usually 10th magnitude and of 0 color index) within each filter and CCD combination in use at each telescope. Similar tables provide the same type of information for the observatory spectrographs as well. The tabulated numeric values, based on actual CCD observations, allow the user, via magnitude, seeing, or filter width, to scale the numbers to a specific observation and predict the S/N expected as a function of integration time.

4.5 Basic CCD data reduction

The process of standard CCD image reduction makes use of a basic set of images that form the core of the calibration and reduction process (Gullixson, 1992). The types of images used are essentially the same (although possibly generated by different means) in imaging, photometric, and spectroscopic applications. This basic set of images consists of three calibration frames – bias, dark, and flat field – and the data frames of the object(s) of interest. Table 4.1 provides a brief description of each image type and Figures 4.2–4.5

Table 4.1. *Types of CCD images*

CCD Image Type	Image Description
Bias	This type of CCD image has an exposure time of zero seconds. The shutter remains closed and the CCD is simply read out. The purpose of a bias or zero frame is to allow the user to determine the underlying noise level within each data frame. The bias value in a CCD image is usually a low spatial frequency variation throughout the array, caused by the CCD on-chip amplifiers. This variation should remain constant with time. The rms value of the bias level is the CCD read noise. A bias frame contains both the DC offset level (overscan) and the variations on that level. The nature of the bias variations for a given CCD are usually column-wise variations, but may also have small row-wise components as well. Thus, a 2-D, pixel-by-pixel subtraction is often required. A single bias frame will not sample these variations well in a statistical fashion, so an average bias image of 10 or more single bias frames is recommended.
	★★★★★
Dark	CCD dark frames are images taken with the shutter closed but for some time period, usually equal to that of your object frames. That is, if one is planning to dark correct a 45 second exposure, a 45 second dark frame would be obtained. Longer dark frames can often be avoided using the assumption that the dark current increases linearly with time and a simple scaling can be applied. However, this is not always true. Dark frames are a method by which the thermal noise (dark current) in a CCD can be measured. They also can give you information about bad or "hot" pixels that exist as well as provide an estimate of the rate of cosmic ray strikes at your observing site. Observatory class CCD cameras are usually cooled with LN2 to temperatures at which the dark current is essentially zero. Many of these systems therefore do not require the use of dark exposure CCD frames in the calibration process. Thermoelectrically cooled systems are not cooled to low enough temperatures such that one may ignore the dark current. In addition, these less expensive models often have poor temperature stability allowing the dark current to wander a bit with time. Multiple darks

Table 4.1. *(cont.)*

CCD Image Type	Image Description
	averaged together are the best way to produce the final dark calibration frame. Note that if dark frames are used, the bias level of the CCD is present in them as well, and therefore separate bias frames are not needed.
Flat Field	Flat field exposures are used to correct for pixel-to-pixel variations in the CCD response as well as any nonuniform illumination of the detector itself. Flat fields expose the CCD to light from either a dome screen, the twilight sky, the nighttime sky, or a projector lamp in an attempt to provide a high S/N, uniformly illuminated calibration image. For narrow-band imaging, flats are very helpful in removing fringing, which may occur in object frames. Flat field calibration frames are needed for each color, wavelength region, or different instrumental setup used in which object frames are to be taken. A good flat should remain constant to about 1%, with 2% or larger changes being indicators of a possible problem. As with the other calibration frames, at least 5 or more flat fields should be taken and averaged to produce the final flat used for image calibration.
	★★★★★
Object	These are the frames containing the astronomical objects of interest. They are of some exposure length from 1 second or less up to many hours, varying for reasons of type of science, brightness of object, desired temporal sampling, etc. Within each object image pixel is contained contributions from the object and/or sky, read noise, thermally generated electrons, and possibly contributions from cosmic rays. Each pixel responds similarly but not exactly to the incident light, so nonuniformities must be removed. All of the noise and spatial factors are correctable to very low levels via standard CCD reductions as described in the text.

show examples of typical bias, dark, flat field, and object CCD images. Note that a CCD dark frame contains not only information on the level and extent of the dark current but also includes bias level information.

The use of the basic set of calibration images in the reduction of CCD object frames is as follows. First, subtract a mean bias frame (or dark frame

https://doi.org/10.1017/CBO9780511807909.006

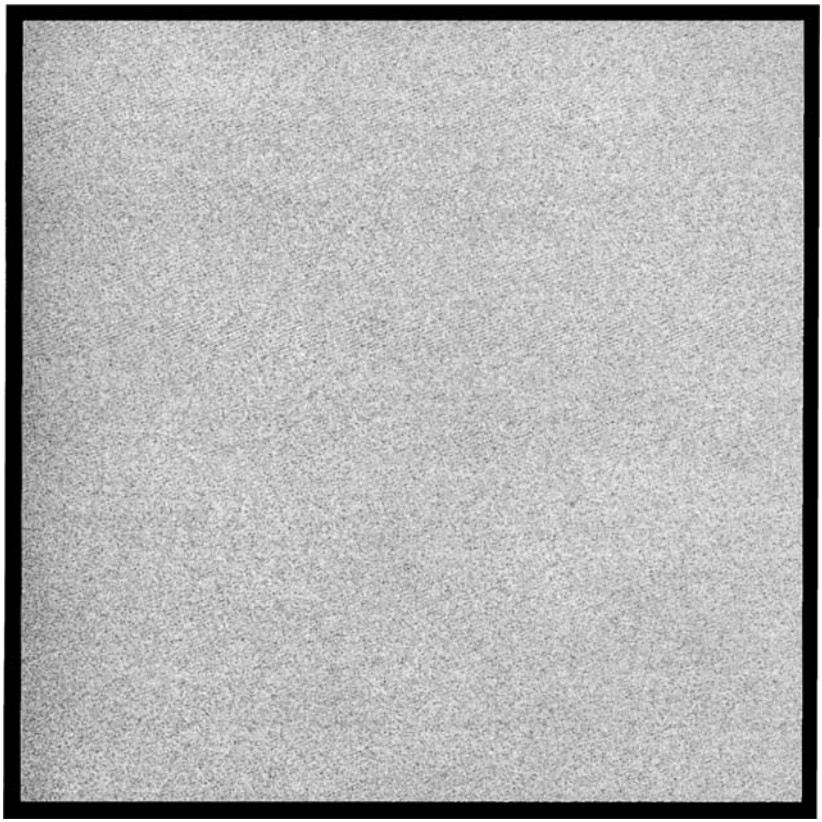

Fig. 4.2. Shown is a typical CCD bias frame. The histrogram of this image was shown in Figure 3.8. Note the overall uniform structure of the bias frame.

if needed[1]) from your object frame. Then, divide the resulting image by a (bias subtracted) mean flat field image. That's all there is to it! These two simple steps have corrected your object frame for bias level, dark current (if needed), and nonuniformity within each image pixel. During the analysis of your object frames, it is likely that the background or sky contribution to the image will need to be removed or accounted for in some manner. This correction for the background sky level in your image frames is performed

[1] The need for dark frames instead of simply bias frames depends entirely on the level of dark current expected during an integration or the stability of the dark current from integration to integration. The first situation depends on the operating temperature of the CCD. LN2 systems have essentially zero dark current, and thus bias frames are all that is needed. Inexpensive and thermoelectrically cooled CCD systems fall into the category of generally always needing dark frames as part of the calibration process.

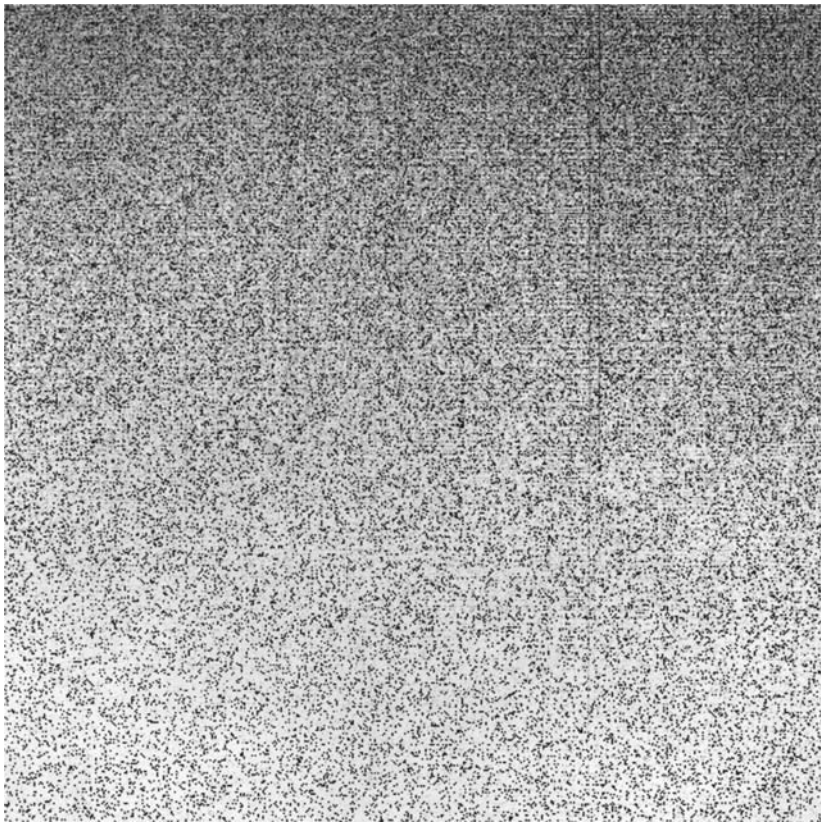

Fig. 4.3. Shown is a typical CCD dark frame. This figure shows a dark frame for a Kodak CCD operating in MPP mode and thermoelectrically cooled. Notice the nonuniform dark level across the CCD, being darker (greater ADU values) on the top. Also notice the two prominent partial columns with higher dark counts, which extend from the top toward the middle of the CCD frame. These are likely to be column defects in the CCD that occurred during manufacture, but with proper dark subtraction they are of little consequence. The continuation of the figure shows the histogram of the dark frame. Most of the dark current in this 180 second exposure is uniformly distributed near a mean value of 180 ADU with a secondary maximum near 350 ADU. The secondary maximum represents a small number of CCD pixels that have nearly twice the dark current of the rest, again most likely due to defects in the silicon lattice. As long as these increased dark current pixels remain constant, they are easily removed during image calibration.

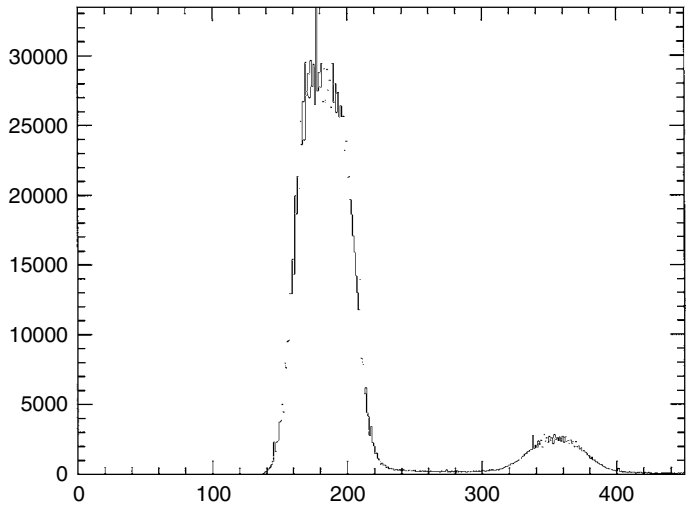

Fig. 4.3. (cont.)

as part of each specific analysis step using "sky" regions in the object frame itself and is not removed or corrected for with some sort of separate "sky" frame. In equational form, the calibration process can be written as

$$\text{Final Reduced Object Frame} = \frac{\text{Raw Object Frame} - \text{Bias Frame}}{\text{Flat Field Frame}},$$

where, again, the flat field image has already been bias subtracted and the bias frame would be replaced by a dark frame when appropriate.

4.6 CCD imaging

This section details issues related to the application of using CCDs to produce images of an extended area of the sky. Examples of this type of CCD observation are multi-color photometry of star clusters, galaxy imaging to isolate star-forming regions within spiral arm structures, deep wide-field searches for quasars, and extended low surface brightness mapping of diffuse nebulae. Use of the areal nature of a CCD introduces some additional issues related to the calibration procedures and the overall cosmetic appearance as any spurious spatial effects will have implications on the output result. We briefly discuss here a few new items that are of moderate concern in two-dimensional imaging and then move on to the topic of wide-field imaging with CCD mosaic cameras.

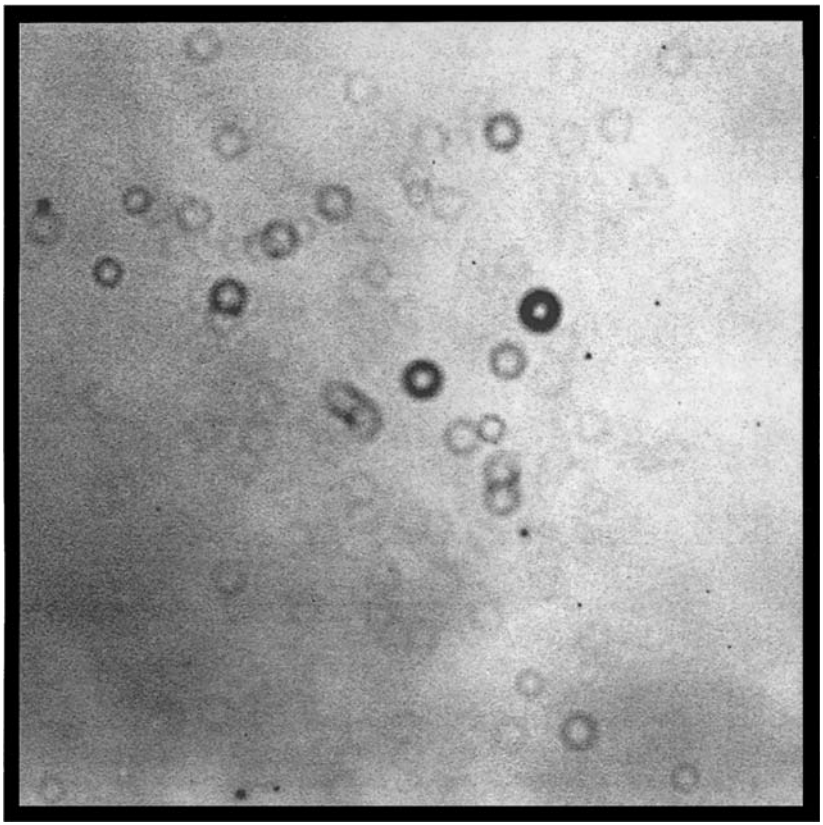

Fig. 4.4. Shown is a typical CCD flat field image. This is an R-band flat field image for a 1024×1024 Loral CCD. The numerous "doughnuts" are out of focus dust specks present on the dewar window and the filter. The varying brightness level and structures are common in flat field images. As seen in the histogram of this image (Figure 4.1) this flat field has a mean level near 6950 ADU, with an approximate dispersion of (FWHM) 400 ADU.

4.6.1 CCD fringing and other cosmetic effects

We mentioned earlier that observations of monochromatic (or nearly so) light can cause a pattern of fringes to occur on a CCD image. These fringes, which are essentially Newton's rings, are caused by interference between light waves that reflect within the CCD or long wavelength light that passes through the array and reflects back into the array. Fringing may occur for CCD observations in the red part of the optical spectrum, when narrow-band filters are used, or if observations are made of a spectral regime (e.g., the I-band) that contains strong narrow emission lines. For a given fringe

cause (e.g., a specific wavelength set of emission lines) the fringe pattern on the CCD remains constant. Figure 4.6 shows a Gemini North GMOS image obtained in a z' filter (central wavelength is near 8800 Å) on a photometric night with no moon but plenty of OH emission. The GMOS detector consists of three EEV red 13.5 micron 6144×4608 CCDs placed next to each other

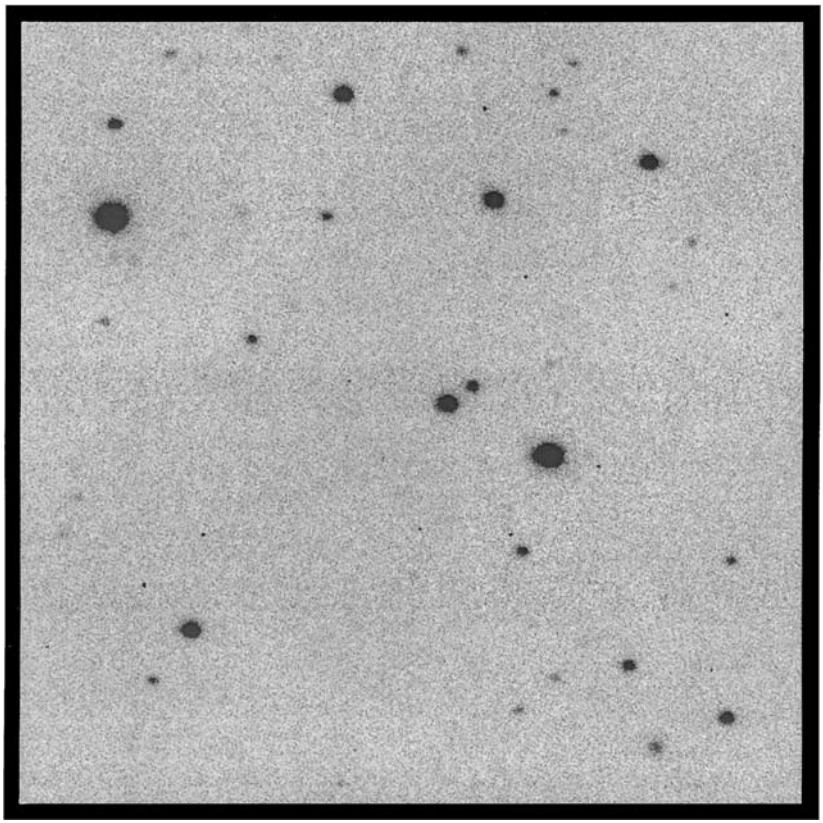

Fig. 4.5. Shown is a typical CCD object frame showing a star field. This image has been properly reduced using bias frame subtraction and division by a flat field image. Note how the background is of a uniform level and distribution; all pixel-to-pixel nonuniformities have been removed in the reduction process. The stars are shown as black in this image and represent R magnitudes of 15th (brightest) to 20th (faintest). The histogram shown in the remainder of the figure is typical for a CCD object frame after reduction. The large grouping of output values on the left (values less than about 125 ADU) are an approximate Gaussian distribution of the background sky. The remaining histogram values (up to 1500 ADU) are the pixels that contain signal levels above the background (i.e., the pixels within the stars themselves!).

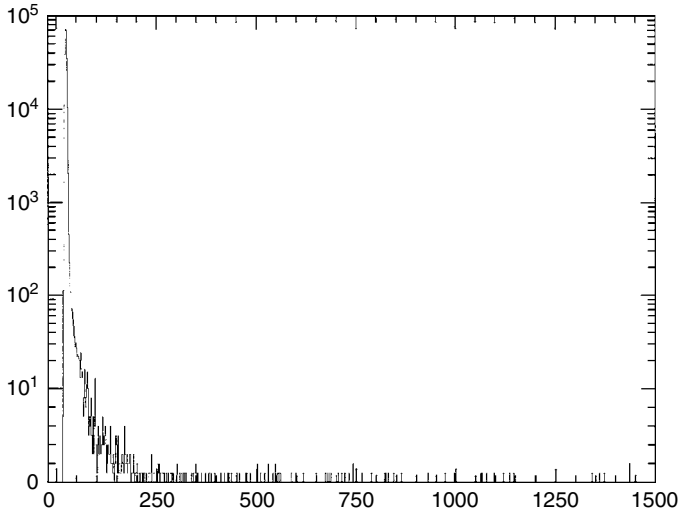

Fig. 4.5. (cont.)

vertically. The frame on the left shows a typical CCD fringe pattern caused by the night sky emission lines while the frame on the right has been defringed. Figure 4.7 presents line plots across typical fringing i' and z' GMOS frames. The typical level of fringing is near $\pm 0.7\%$ in i' and $\pm 2.5\%$ in z'.

The troubling aspect with fringing in CCD data is that it is often the case that the fringe pattern does not occur in the flat field frames (flats contain no emission lines!) or the level of fringing is highly variable throughout the night. Without a pattern match between the flats and the image data, fringe removal will not robustly occur during image calibration, and residual fringes will remain in the final object images. One of the major causes of CCD fringing is the night sky emission lines, which occur in the Earth's upper atmosphere (Pecker, 1970). These night sky lines are mainly attributed to OH transitions in the atmosphere, which are powered by (UV) sunlight during the day. Since they are forbidden transitions they have long decay lifetimes and are very narrow spectrally. In addition, due to upper atmosphere motions, OH concentrations, and their long decay times, these emission lines are highly variable in time and strength, even within a given night. Dealing with fringes that occur in CCD data can be a difficult problem but one for which solutions exist (Broadfoot & Kendall, 1968; Wagner, 1992). Observations with newly defined moderate-band filters that lie between the OH transitions is one such example.

Additionally, cosmetic effects such as bad pixels, hot pixels (LEDs), stuck bits, or dead columns can be present and can mar a CCD image. Not only do these

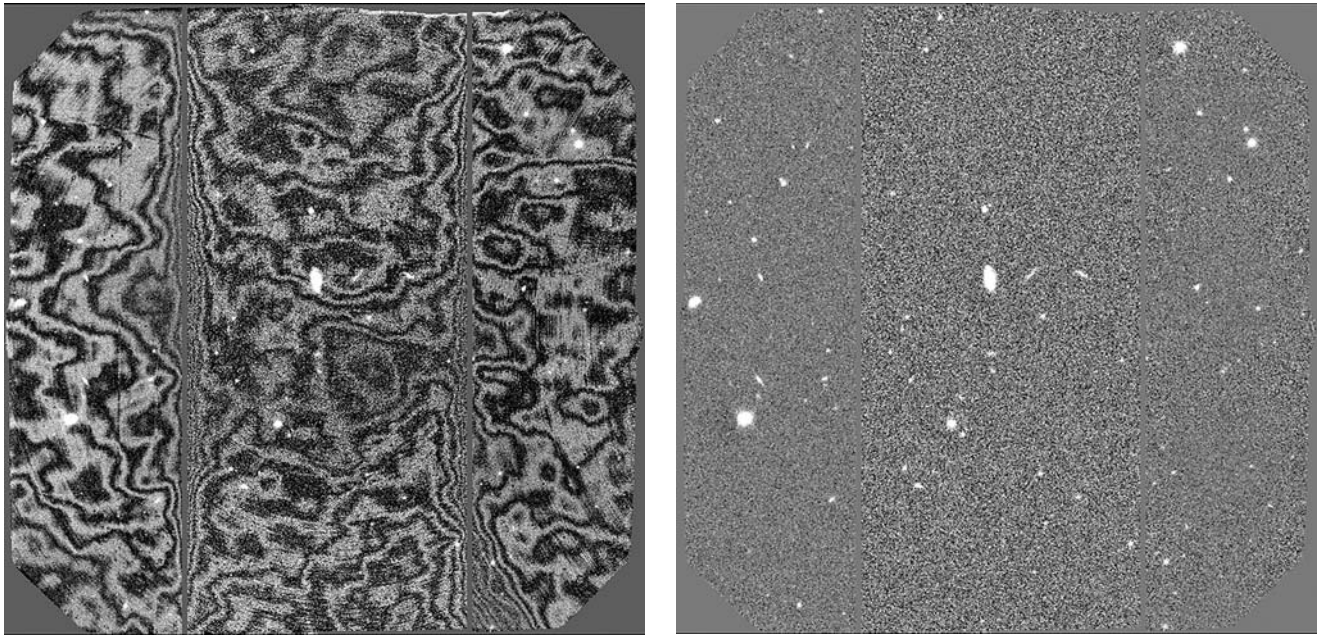

Fig. 4.6. Gemini North GMOS CCD fringe frame (left) and reduced, defringed, frame (right). The night was photometric and near new moon but had OH emission present. Notice that the 1–2% fringes can cross over objects of interest but are mostly fully removed during reduction.

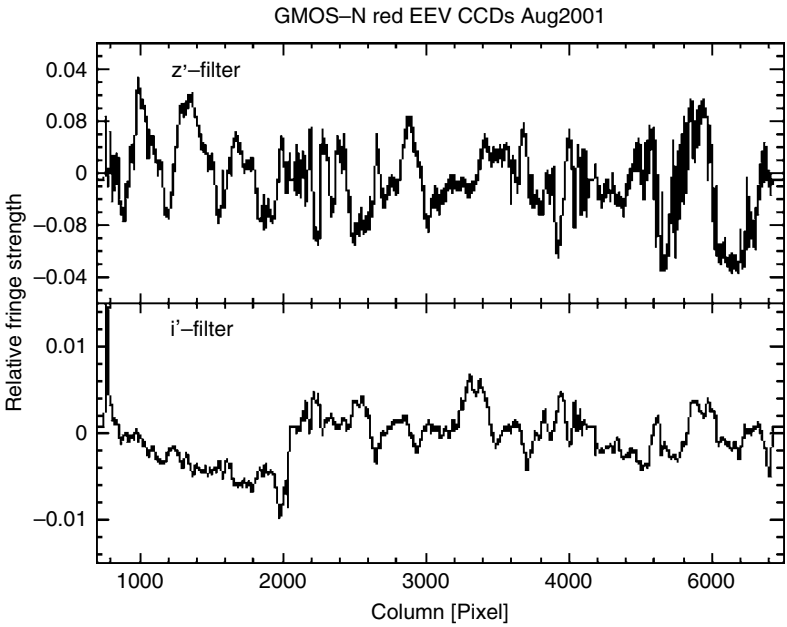

Fig. 4.7. Line plots across the unprocessed GMOS i' and z' images. The plots have been normalized such that the mean image level is zero and the fringe level can be seen to be both positive and negative deviations from this level. The i' fringing is about 0.7% while the z' fringing is near 2.5%.

flaws spoil the beauty of the two-dimensional data, they can cause problems during calibration and analysis by hindering software processes and not allowing correct flux estimates to be made for the pixels that they affect. Procedures for the identification and removal of, or correction for these types of problems can be applied during image calibration and reduction. They are specialized reduction tasks, which depend on the desired output science goals and generally are specific to a particular CCD, instrument, or type of observation being made. Most observatories provide solutions to such fixed flaws. One example is a bad pixel map, which consists of an "image" of 0s and 1s with 0s at the locations of bad columns or other regions of bad pixels. These maps are used by software in the reduction process to eliminate and fix offending CCD problems. A complete discussion of all of these topics lies beyond our space limitations but the interested reader will find discussions of such corrections in Djorgovski (1984), Janesick *et al.* (1987a), Gilliland (1992), Gullixson (1992), Massey & Jacoby (1992), and numerous specific instrument manuals and reference papers concerning the finer points of specific CCD related issues (see Appendix A).

4.6.2 Tip-tilt corrections

The Earth's atmosphere causes a blurring of an image and thus a reduction in image quality during an observation. A solution that often eliminates nearly 70–80% of this effect is the use of adaptive optics to perform low order tip-tilt corrections. Mechanical tip-tilt systems exist today at many observatories and consist of a guide star sensor of some type (avalanche photodiodes (APDs) or a small CCD) and a small optical mirror that can tip and tilt rapidly. The sensor receives light from a bright guide star in the field of view (or a laser guide star) during an observation and the quality (mainly the x,y position) of the image observed by the sensor is assessed. A fast feedback is established by which any movement in the guide star is measured and a correction tip-tilt signal is sent to the moveable mirror.

Systems of this type have small fields of view (~2–4 arcminutes) and can only work well if a bright guide star is present of if the telescope is equipped with a laser beacon. Orthogonal transfer CCDs were developed to provide nonmechanical tip-tilt corrections. The OTCCD camera OPTIC (Tonry *et al.*, 1997) has four guide regions (at the ends of the CCDs) and four associated science regions. Up to four stars that fall in the guide regions are used for tip-tilt correction. These stars are read out fast (typically 10–20 Hz), assessed, and a tip-tilt correction signal is fed back to the science regions of the CCDs during the integration. OTCCDs can shift charge on the array in both x and y directions and use this property to provide fast tip-tilt correction in the science image. This same type of feedback can also simultaneously correct for telescope drive errors and wind shake (see Tonry *et al.*, 1997, Howell *et al.*, 2003).

The new generation of OTCCD, the OTAs (see Figures 2.7 and 2.8), will extend the tip-tilt correction ability. They allow use of any of the individual OTCCDs within the 8×8 array to be used as a guide region. Additionally, the ability to tip-tilt correct an image can be extended to an arbitrarily large field of view as each part of the OTCCD array corrects itself locally. The WIYN observatory is building a one-degree imager that will provide tip-tilt corrections across the entire 1° field of view. The Pan-STARRS project is developing a similar imager that will cover a 3° field (Jacoby *et al.*, 2002, Tonry *et al.*, 2002).

4.6.3 Wide-field CCD imaging

With the advent of large-footprint CCDs and the construction of CCD mosaic arrays containing many chips, wide-field imaging is becoming one of the major applications in astronomy today. One of the major efforts in observational astronomy today is large field of view, multi-color imaging of the

https://doi.org/10.1017/CBO9780511807909.006

sky. Large surveys such as the Sloan digital sky survey (SDSS) and the two-micron all sky survey (2MASS) are complete and their contribution to astronomy has been amazing. New types of objects, large, very complete samples, and follow-up spectroscopy have shown that imaging surveys can provide tremendous new information.

Temporal variation of the objects in the night sky (both known and unknown) is an additional parameter becoming an integral part of modern imaging surveys. At least six very ambitious wide-field imaging projects are well underway to complement the ten or so, 0.5–1.0° field of view imagers already in action. Table 4.2 lists a few examples of modern wide-field CCD imaging cameras available to the astronomer today as well as those planned to be built and on-line in the next decade. Wide-field imagers of even five years ago consisted of four large format CCDs and required minutes for readout and often days for data reduction. Modern wide-field cameras consist of dozens of CCDs, readout very fast (and will get faster with estimates of 2–4 s), and pass through automated software pipelines in a matter of hours. Figures 4.8–4.10 show two currently working large CCD mosaic cameras plus the planned Pan-STARRS OTCCD camera.

MegaCam on the CFHT was the first operational wide-field, megapixel CCD imager (Boulade *et al.*, 1998) starting science operation in 2002. Today, the Large Synoptic Survey Telescope (LSST) project is the most ambitious of the currently planned wide-field imagers. This special purpose imaging telescope will have a camera containing gigapixels of CCD real estate and image an area of nearly ten square degrees at a time. The LSST camera (see Table 4.1) will likely use an array of 1K or 2K CMOS or CCD ASIC devices. ASIC (Application Specific Integrated Circuits) devices are special purpose production circuits made with a number of non-changeable specific modes built directly into the chip. As such, ASIC devices are often higher in efficiency but somewhat limited in expandability for use other than what they were designed for. An example of a common ASIC device is the computer chip residing under the hood of most modern automobiles. The LSST will image the entire sky every few nights and the amount of data produced will run into the petabytes.

Astronomers are beginning to become different types of observers. Virtual on-line databases, such as the National Virtual Observatory (NVO) will soon sponsor the ability for world-wide access to a tremendous amount of data. Preliminary versions of the web tools and software exist today and with many new CCD imagers available and ever larger ones coming along, there promises to be no shortage of data to sift through and extract scientific research projects from. One downside to this type of observational work is

Table 4.2. *Some Present and Planned Large Telescope CCD Imagers (∗ marks planned imagers)*

Name	Telescope	Field of View	Focal Plane CCDs	Pixel Size (microns)	Pixel Scale (″/pix)	Website
MageCam	CFHT	0.92 sq. degrees	$40-2048\times4612$ E2V	13.5	0.185	http://www.cfht.hawaii.edu/Instruments/Imaging/Megacam/
QUEST	Palomar 48″ Schmidt	16 sq. degrees	$112-600\times2400$ Sarnoff	13	~ 1.5	http://www.astro.caltech.edu/~george/pq/
SUPRIME	Subaru	0.24 sq. degrees	$10-2048\times4096$ MIT/LL	15	0.2	http://www.naoj.org/Observing/Instruments/SCam/
Mosaic	KPNO/CTIO 4-m	0.36 sq. degrees	$8-2048\times4096$ SITe	15	0.26	http://www.noao.edu/kpno/mosaic
MegaCam	MMT	0.16 sq. degrees	$32-2048\times4096$ E2V	15	0.087	http://cfa-www.harvard.edu/~bmcleod/Megacam/
Dark Energy Camera∗	CTIO 4-m	2.9 sq. degrees	$70-2048\times4096$ LBL	15	0.28	http://www.fnal.gov/pub/
OmegaCam*	VST	1.0 sq. degrees	$32-2048\times4096$ E2V	15	0.21	http://www.eso.org/instruments/omegacam/
One Degree Imager∗	WIYN	1.0 sq. degrees	(OTA) $60-3840\times3952$ STA/Dalsa	12	0.11	http://www.noao.edu/wiyn/ODI/
Pan-STARRS∗	1.8-m	7.0 sq. degrees	(OTA) $60-4096\times4096$ MIT/LL	12	0.3	http://pan-starrs.ifa.hawaii.edu/public/index.html
Kepler∗ (Spacecraft)	1.0-m Schmidt	105 sq. degrees	$42-2200\times1024$ E2V	27	4	http://www.kepler.arc.nasa.gov/
LSST Camera∗	LSST	9.6 sq. degrees	3 Gigapixels LBL	10	0.2	http://www.lsst.org/lsst_home.shtml

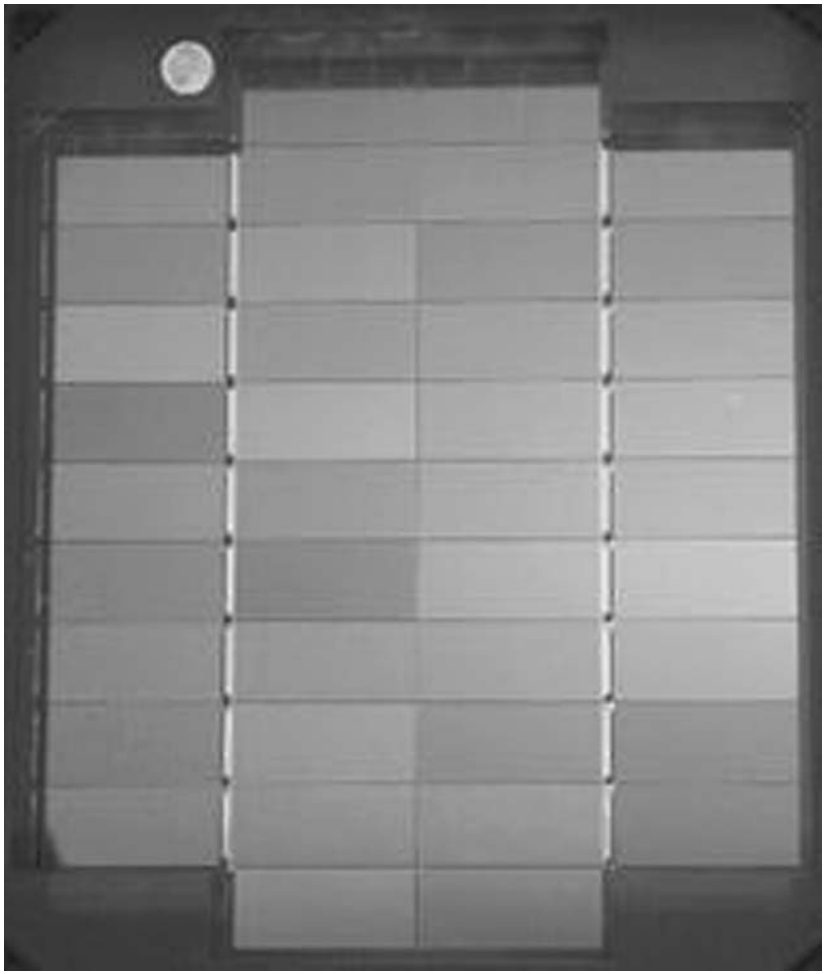

Fig. 4.8. Photograph of the CCDs used in the CFHT MegaCam. Forty large format E2V CCDs are used in this camera, which can image a field of view of nearly 1×1 degree on the sky.

that the virtual observer will only be able to get the data that were taken and they may or may not suit their needs. So don't stop thinking of your own observational projects or planning to go to a telescope to collect your own data just yet.

Wide-field CCD mosaic imagers provide a tremendous amount of information (and data) to be collected in one exposure. The soon-to-be-operating OmegaCam on the VLT survey telescope (VST), for example, will produce

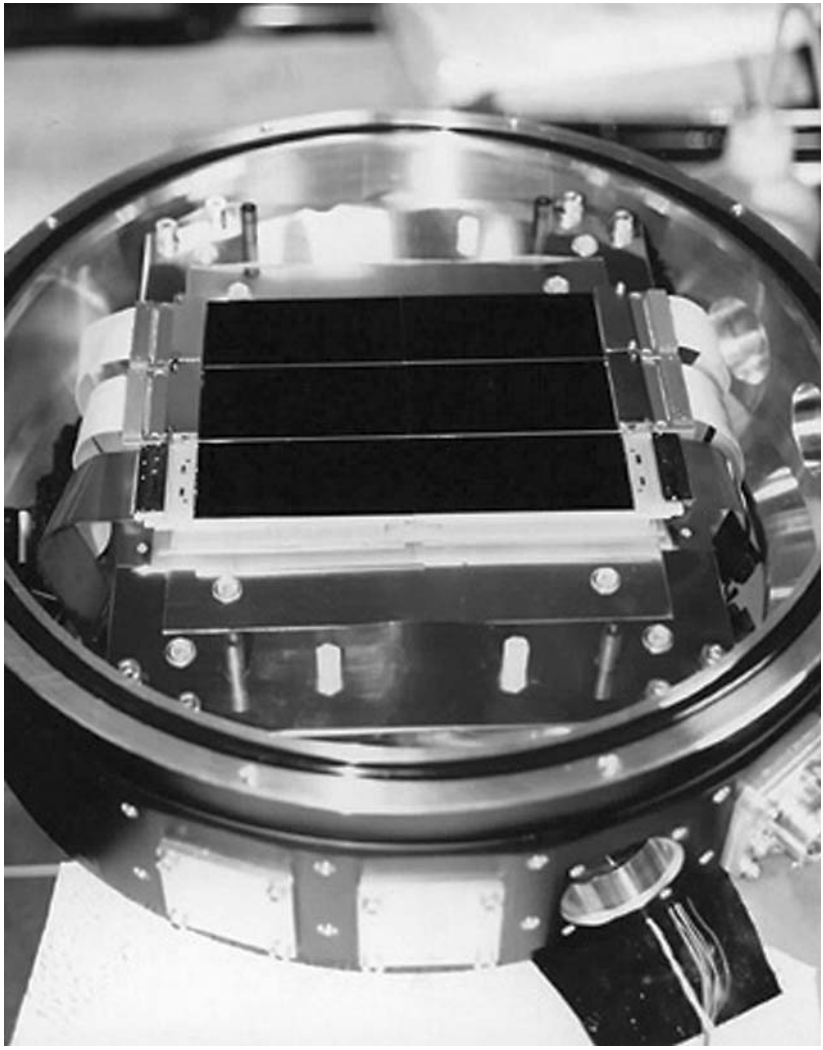

Fig. 4.9. A view of the Subaru SuPrime CCDs mounted in the camera dewar. This camera images a field of view of $\sim 0.5°$ on a side using ten 2048×4096 MIT/LL CCDs.

over 4200 Mb of data in one exposure! CCD mosaic arrays are pioneering new scientific advances and driving astronomical technology such as read-out, CCD controllers, and data storage. These larger CCD arrays are also being enabled by faster computational ability and increased effort in software and hardware development. Astronomers have been making a transition from

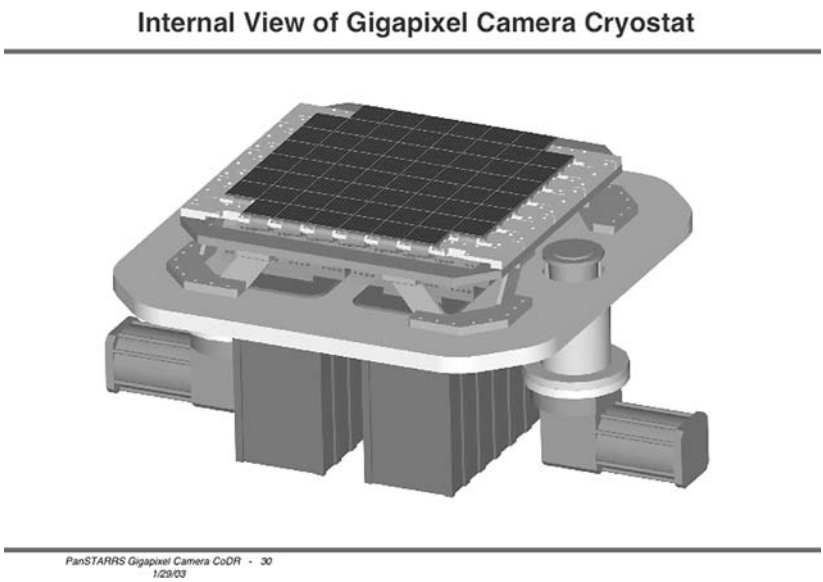

Fig. 4.10. Engineering drawing of one of the four Pan-STARRS imagers currently under construction. This camera will use sixty OTAs to cover a 7 square degree field of view.

single researchers and few night runs at a telescope, to large collaborations that build instruments and telescopes, to the production of extensive non-proprietary databases. Financial constraints and enormous complexity are the prime drivers of this new research model. Physicists went down this road many years ago and we often joke about their papers having less text in the science portion then the two pages that list the 200 authors. Astronomy is going in this direction and the new generation of large, expensive CCD imagers are leading the way.

The efficiency of a large-area survey can be estimated by the metric

$$\epsilon = \Omega D^2 q,$$

where Ω is the solid angle of the field of view, D is the diameter of the telescope, and q is the total throughput quantum efficiency of the instrument assuming that the seeing disk is resolved. One can see that the time needed for completion of a survey to a given brightness limit depends inversely on ϵ.

Using wide-field CCD imagers leads to the inevitable result that new issues of calibration and data reduction must be developed. For example, when the field of view of a large-area CCD (whether a single large CCD

with a wide-field of view or an array of chips) approaches $\sim 0.5°$ in size, differential refraction of the images across the field of view of the CCD begins to become important. Color terms therefore propagate across the CCD image and must be corrected for to properly determine and obtain correct photometric information contained in the data.

CCD observations that occur through uniform thin clouds or differential measures essentially independent of clouds are often assumed to be valid, as it is believed that clouds are grey absorbers and that any cloud cover that is present will cover the entire CCD frame. Thus flux corrections (from, say, previous photometric images of the same field) can be applied to the nonphotometric CCD data, making it usable. Large-field CCD imaging can not make such claims. A one or more square degree field of view has a high potential of not being uniformly covered by clouds, leading to unknown flux variations across the CCD image.

Observations of large spatial areas using CCD mosaics also necessitate greater effort and expense in producing larger filters, larger dewar windows, and larger correction optics. Variations of the quality and color dependence of large optical components across the field of view are noticeable and their optical aberrations will cause point-spread function (PSF) changes and other effects over the large areas imaged with wide-field CCDs. Production of large, high quality optical components is a challenge as well. For example, recent estimates for the cost of a single 16 to 20-inch square astronomical quality glass filter are in the range of $50 000–200 000.

The use of large-format CCDs or CCD mosaics on Schmidt telescopes is increasing and such an imager provides a good example of the type of PSF changes that occur across the field of view (see Figure 4.11). Coma and chromatic aberrations are easily seen upon detailed inspection of the PSFs, especially near the corners or for very red or blue objects whose peak flux lies outside of the color range for which the optics were designed. Thus, for wide-field applications, such as that represented in Figures 4.8–4.10, the typical assumption that all the PSFs will be identical at all locations within the field of view must be abandoned.

A more subtle effect to deal with in wide-field imaging is that of the changing image scale between images taken of astronomical objects and those obtained for calibration purposes. For example, a dome flat field image taken for calibration purposes will not have exactly the same image scale per pixel over the entire CCD image as an object frame taken with the same CCD camera, but of an astronomical scene. Also, how one maps the light collected per (non-equal area) pixel in the camera to a stored image in say RA and DEC is a tessellation problem to be solved.

https://doi.org/10.1017/CBO9780511807909.006

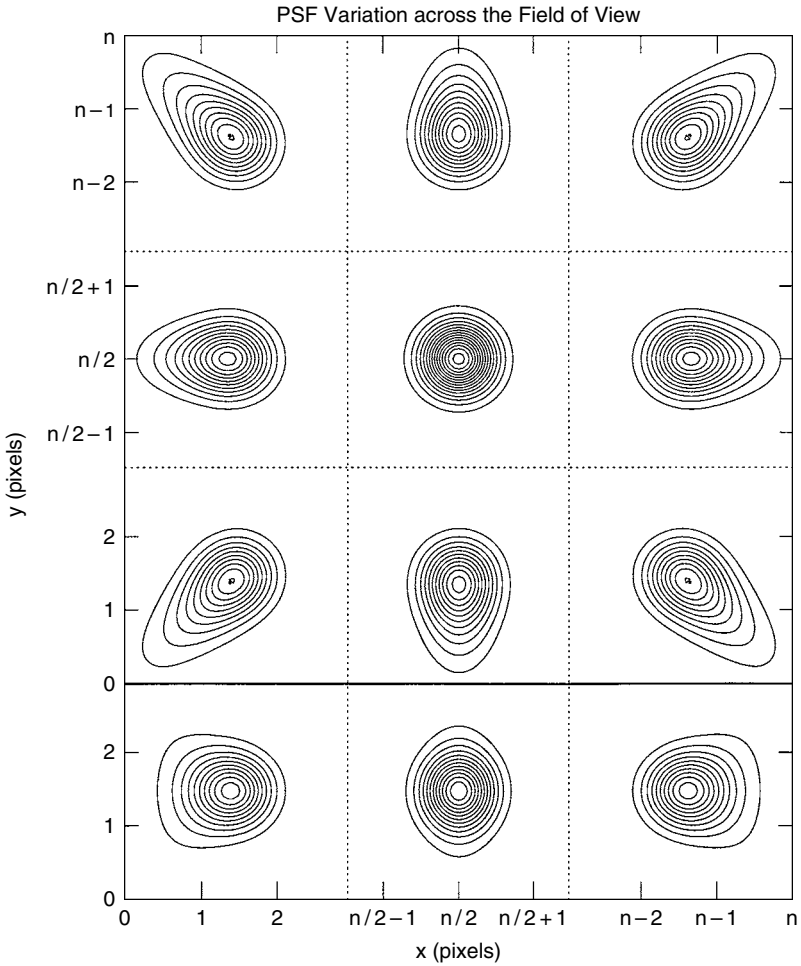

Fig. 4.11. PSF variations for a star imaged at nine locations within the field of view of a large mosaic CCD camera placed at the focal plane of a Schmidt telescope. Only the center of the field has a circular, symmetric PSF while the other positions show extended tails due to optical abberations and chromatic effects. The three PSFs at the bottom of the figure are column sums of the PSFs vertically above them. From Howell *et al.* (1996).

As with previous new advances in CCD imaging, wide-field imaging has issues that must be ironed out. However, this exciting new field of research is still in its infancy and those of you reading this book who are involved in such work are the ones who must help determine the proper data collection and reduction procedures to use.

4.6.4 CCD drift scanning and time-delay integration

The standard method of CCD imaging is to point the telescope at a particular place in the sky, track the telescope at the sidereal rate, and integrate with the detector for a specified amount of time. Once the desired integration time is obtained, the shutter is closed and the CCD is readout. For telescopes incapable of tracking on the sky or to obtain large areal sky coverage without the need for complex CCD mosaics, the techniques of CCD drift scanning and time-delay integration were developed (McGraw, Angel, & Sargent, 1980; Wright & Mackay, 1981).

Drift scanning consists of reading the exposed CCD at a slow rate while simultaneously mechanically moving the CCD itself to avoid image smear. The readout rate and mechanical movement are chosen to provide the desired exposure time. Each imaged object is thus sampled by every pixel in the column thereby being detected with the mean efficiency of all pixels in the column. Nonuniformities between the pixels in a given column are thus eliminated as each final pixel is, in essence, a sum of many short integrations at each pixel within the column. Cross column efficiency differences are still present but the final image can now be corrected with a one-dimensional flat field. Drift scanning also has the additional advantage of providing an ideal color match to background noise contributions, unavailable with dome flats. Very good flat fielding of a traditional image might reach 0.5 or so percent, while a good drift scanned CCD image can be flattened to near 0.1 percent or better (Tyson & Seitzer, 1988). Drift scanning has even been accomplished with IR arrays (Gorjian, Wright, & Mclean, 1997).

Time-delay integration or TDI is a variant on the drift scanning technique. In TDI, the CCD does not move at all but is readout at exactly the sidereal rate. This type of CCD imaging is necessary if astronomical telescopes such as transit instruments (McGraw, Angel, & Sargent, 1980) or liquid mirror telescopes (Gibson, 1991) are to be used. The same flat fielding advantages apply here as in drift scanning but the integration time per object is limited by the size of the CCD (i.e., the time it takes an object to cross the CCD field of view). For a 2048×2048 CCD with 0.7 arcsec pixels, the integration time would be only 96 seconds at the celestial equator. Rescanning the same area could be performed and co-added to previous scans as a method of increasing the exposure time, but time sampling suffers.

TDI is mechanically simple, as nothing moves but the electrons in the CCD. This charge movement has been termed electro-optical tracking. Large sky regions can be surveyed, albeit to shallow magnitude limits, very quickly using TDI. Overhead time costs for TDI only consist of the "ramp up" time,

https://doi.org/10.1017/CBO9780511807909.006

that is, the time needed for the first objects to cross the entire field, and the scan time. Using our same 2048×2048 CCD as in the example above, we find that a 23 arcsec by 3 degree long strip of the sky at the celestial equator can be scanned in about 2–3 minutes compared with the nearly 25 minutes required if pointed observations of equivalent integration are used.

Although drift scanning and TDI are seemingly great solutions to flat fielding issues and offer the collection of large datasets, drift scanning requires the CCD to move during the integration with very precise and repeatable steps. This is quite a mechanical challenge and will increase the cost of such an instrument over that of a simple CCD imager. In addition, both techniques suffer two potential drawbacks (Gibson & Hickson, 1992). Images obtained by drift scanning and TDI techniques have elongated PSFs in the east–west direction. This is due to the fact that the rows of the CCD are shifted discretely while the actual image movement is continuous. We note here that objects seperated by even small declination differences (i.e., one CCD field of view) do not have the same rate of motion. The resulting images are elongated east–west and are a convolution of the seeing with the CCD pixel sampling.

TDI imagery contains an additional distortion in the north–south direction due to the cuvature of an object's path across the face of the CCD (if imaging away from the celestial equator). This type of distortion is usually avoided in drift scan applications as the telescope and CCD tracking are designed to eliminate this image smearing. This sort of mechanical correction can not be applied to TDI imaging.

These image deformations have been studied in detail (Gibson & Hickson, 1992) and are seen to increase in magnitude for larger format CCDs or declinations further from the celestial equator. For example, at a declination of $\pm 30°$, a 1 arcsec per pixel CCD will show an image smear of about 6 pixels. One solution to this large image smear is to continuously reorient the CCD through rotations and translations, such that imaging scans are conducted along great circles on the sky rather than a polar circle or at constant declination. Such a mechanically complex device has been built and used for drift scanning on the 1-m Las Campanas telescope (Zaritsky, Shectman, & Bredthauer, 1996). Another solution is the development of a multilens optical corrector that compensates for the image distortions by tilting and decentering the component lenses (Hickson & Richardson, 1998).

A few telescopes have made good use of the technique of drift scanning or TDI, providing very good astronomical results. Probably the first such project was the Spacewatch telescope (Gehrels *et al.*, 1986) built to discover and provide astrometry for small bodies within the solar system. Other notable

examples are the 2-m transit telescope previously operated on Kitt Peak (McGraw, Angel, & Sargent, 1980) and a 2.7-m liquid mirror telescope currently running at the University of British Columbia (Hickson *et al.*, 1994). This latter telescope contains a rotating mercury mirror and images a 21-arcminute strip of the zenith with an effective integration time of 130 seconds. Using TDI, a typical integration with this liquid mirror telescope reaches near 21st magnitude in R and continuous readout of the CCD produces about 2 Gb of data per night.

Present-day examples of telescopes employing drift scanning and TDI techniques are the QUEST telescope (Sabby, Coppi, & Oemler, 1998), the Palomar QUEST imager (see Table 4.2) and the Sloan digital sky survey (Gunn *et al.*, 1998). The QUasar Equatorial Survey Team (QUEST) telescope is a 1-m Schmidt telescope that will provide UBV photometry of nearly 4000 square degrees of the sky to a limiting magnitude of near 19. The focal plane will contain sixteen 2048×2048 Loral CCDs arranged in a 4×4 array. The telescope is parked and the CCDs are positioned such that the clocking (column) direction is east–west and the readout occurs at the apparent sidereal rate. Each object imaged passes across four CCDs covered, in turn, with a broadband V, U, B, and V filter. The effective integration time (i.e., crossing time) is 140 seconds, providing nearly simultaneous photometry in U, B, and V.

As we have seen above, a problem with drift scanning is that the paths of objects that drift across the imager are not straight and they can cross the wide-field of view with different drift rates. We have discussed a few solutions to these issues, and in the QUEST project (Sabby, Coppi, & Oemler, 1998) we find another. The CCDs are fixed, in groups of four, to long pads lying in the north–south direction. These pads can pivot independently such that they align perpendicular to the direction of the stellar paths. The CCDs are also able to be clocked at different rates, with each being readout at the apparent sidereal rate appropriate for its declination.

The Sloan digital sky survey (SDSS) is a large-format mosaic CCD camera consisting of a photometric array of thirty 2048×2048 SITe CCDs and an astrometric array of twenty four 400×2048 CCDs (see Figure 4.12). The photometric CCDs are arranged in six columns of five CCDs each, providing essentially simultaneous five-color photometry of each image object. The astrometric CCDs are mounted in the focal plane above and below the main array and will be used to provide precise positional information needed for the follow-up multi-fiber spectroscopy. The SDSS uses a 2.5-m telescope located in New Mexico to image one quarter of the entire sky down to a limiting magnitude of near 23.

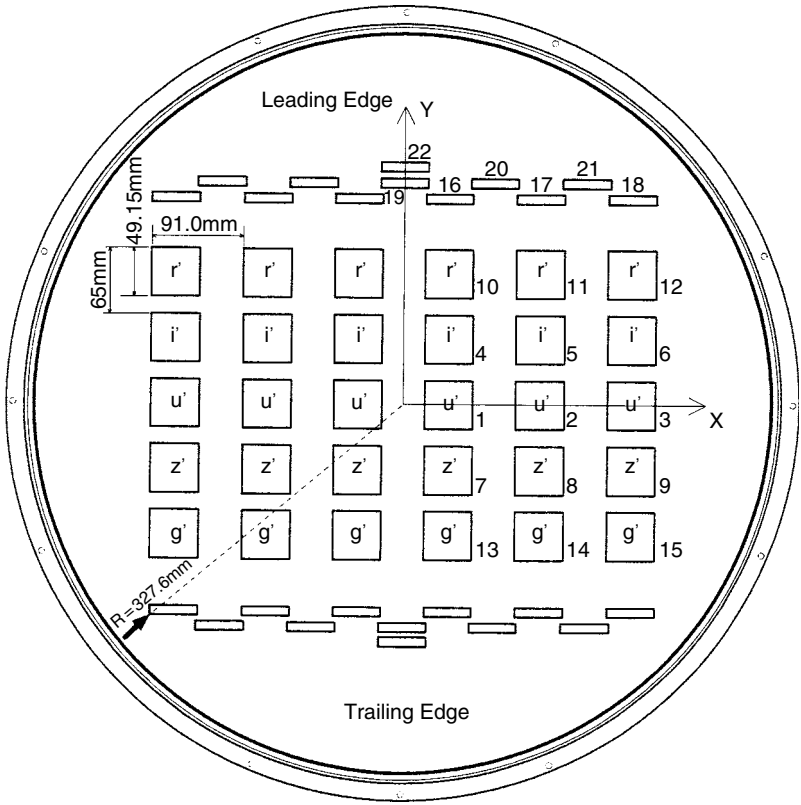

Fig. 4.12. The optical layout within the dewar of the Sloan digital sky survey CCD imager. The right side of the figure labels the CCDs as to their function; 1–15 are photometric CCDs, 16–21 are astrometric CCDs, and 22 (top and bottom) are focus CCDs. The left side gives the dimensions of the array. The labels r'–g' denote the five separate intermediate band filters, each a single piece of glass covering all six horizontal CCDs. The scan direction is upward causing objects to traverse the array from top to bottom. From Gunn *et al.* (1998).

TDI scans along great circles are used by the SDSS to image a region of the sky 2.5° wide. Using five intermediate band filters, covering 3550 Å to 9130 Å, scanning at the sidereal rate provides an effective integration per color of 54 seconds with a time delay of 72 seconds between colors caused by CCD crossing time and chip spacing. Complete details of the SDSS, too lengthy for presentation here, can be found in Gunn *et al.* (1998). Other projects of a similar nature are discussed in Boulade *et al.* (1998), Gunn *et al.* (1998), and Miyazaki *et al.* (1998). The SDSS prime survey is complete and much of the data are already available (see Appendix B).

4.7 Exercises

1. Derive the first two equations of Chapter 4.
2. What focal length (f-ratio) of telescope is best if your observational requirements need a plate scale of about one tenth of an arcsec/pixel? How does your answer depend on the type of CCD used? What is the f-ratio of a typical present-day large reflecting telescope?
3. Design an experiment to obtain a good flat field image, that is, one that will allow you to measure the pixel-to-pixel variations to 1%. How might your experiment differ if you were to make the measurements in the red? In the blue? Of the night sky?
4. What are the differences between a sky flat and a dome flat? Which is easier to obtain? Which provides the better flat field?
5. What are the flat fielding requirements needed for point source photometry? For extended object spectroscopy? For extended object imaging? How might you accomplish each of these?
6. Using the method outlined in Section 4.3, determine the gain and read noise for a CCD you work with.
7. Using the equations presented in Section 4.4, calculate the individual noise contribution per pixel from read noise, sky background, and dark current given the following conditions. You are using an E2V CCD at operating temperature (as described in Table 3.2) and have obtained a 1200 second exposure on a full moon night using a Johnson V filter. (Note: You will have to estimate the sky brightness (see an observatory website for such details), plate scale, and band-pass of your observation.) Plot your results. Which noise source is the greatest? How might you eliminate it?
8. Derive the signal-to-noise equation.
9. Describe an observational setup for which a 15th magnitude galaxy is a bright source. Do the same for a faint source.
10. Work through the example S/N calculation given in Section 4.4.
11. Answer the question posed in the footnote on page 76.
12. Derive the expression for the integration time needed to achieve a specific S/N as given at the end of Section 4.4.
13. Produce a flow chart of a typical reduction procedure for CCD imaging observations. Clearly show which types of calibration images are needed and when they enter into the reduction process.
14. Why do you divide object frames by a flat field calibration image instead of multiplying by it?

15. Look at Figure 4.4. If the doughnuts are due to out-of-focus dust, how might you be able to use their size or shape to tell if that dust was on the dewar window or on a filter high above the CCD dewar?
16. Using information on the wavelengths and strengths of night sky emission lines (see e.g., Broadfoot and Kendall, 1968, Pecker, 1970, or observatory websites), discuss which broad-band Johnson filters are likely to be affected by these lines. How might one design an observational program that uses these filters but lessens the effect of the night sky lines?
17. Using the physical principles of Newton's Rings, quantitatively describe CCD fringing providing a relationship between the CCD thickness and the wavelength observed.
18. Discuss how OTCCDs can provide tip-tilt corrections over an arbitrary field of view. Why can mechanical tip-tilt systems not do this?
19. Using the expression given for the efficiency of a large area survey, calculate the efficiency for each imaging program listed in Table 4.2. How does the LSST project compare to the rest? How do your values compare with a survey using a 4-m f/1.5 telescope able to image onto a 14×14 inch photographic plate?
20. Design an observational experiment to map galaxy clusters using a CCD system that operates in drift scanning mode. Discuss the details of observational strategy, integration times, instrument design, and calibration. Where would you locate your survey telescope and why is this important? How does this type of observation program compare with a similar one that uses a conventional point-and-shoot CCD system?
21. Read the description of the Sloan survey given in Gunn *et al.* (1998). Discuss why this survey is important to astronomy. Can you think of any improvements you would make to the methods used if you were designing the survey?